

Improved Vehicle Performance Using Combined Suspension and Braking Forces

Andrew Alleyne

Department of Mechanical and Industrial Engineering
University of Illinois, Urbana-Champaign
Urbana, IL 61801

Abstract

This paper investigates the integration of various subsystems of an automobile's chassis. The specific focus of this research is the integration of active suspension components with anti-lock braking (ABS) mechanisms. The performance objective for the integrated approach is defined as a reduction in braking distance over just anti-lock brakes. A two degree of freedom Half Car vehicle model is developed along with models for a hydraulic active suspension and an ABS system. For both subsystems, actuator dynamics are included. Individual controllers are developed for the subsystems and a governing algorithm is constructed to coordinate the two controllers. Simulations of the integrated controller and an ABS system demonstrate a significant increase in performance.

1. Introduction

The past decade has seen large advances in the electronic control of various vehicle chassis components. As the speed to cost ratio of computing has dramatically increased, so have the applications to automotive control. Presently, most of the major vehicle chassis components have some type of controller available to them. Anti-lock Braking (ABS) Systems [3,12,14] and Traction Control (TC) Systems [13,16] are now standard in the industry. Additionally, a large amount of work has been done in the area of Active Suspensions [1,2,5]. To date, there have been some preliminary investigations into the coordination of these systems to generate an integrated approach to the control of Vehicle Dynamics. In many of these early studies steering systems are included. The fundamental principle underlying these efforts is the coordination of forces at the vehicle tires shown in Figure 1.1.

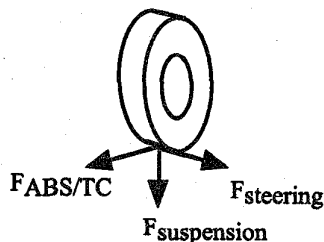


Figure 1.1
Vehicle Tire Forces

Roppenecker & Wallentowitz [15] outline several available strategies for this systems integration approach. Matsumoto et al [9] consider the effects of braking force distribution control on yaw rate and vehicle control. Matsumoto & Tomizuka [10] briefly investigate the combination of braking control with steering inputs for steady state maneuvering involving independent lateral velocity and yaw rate control. Xia & Law [18] consider the combination of steering and braking inputs on Four Wheel Steer (4WS) vehicles. Kimbrough et al [8] also consider the effects of braking and steering inputs, particularly with respect to combination vehicles (tractor-trailer types). Dreyer et al [4] consider the integration of Semi-Active suspensions with ABS/TC and conclude that improved vehicle braking performance could be achieved.

The concept of integrating an Active Suspension with an ABS system has not yet been investigated. This paper will outline an initial study on the coordination of these two systems. The goal is to reduce the vehicle braking distance relative to a system equipped solely with an ABS system. This is achieved by increasing the vertical tire force exerted normal to the road surface in coordination with the application of the ABS. The Active Suspension will be the tool used to achieve the regulation of the normal force. The analysis will be carried out on a two degree of freedom Half Car model.

The rest of the paper is organized as follows. Section 2 introduces the dynamics of the system, including the Half Car model, the Active Suspension model, and the ABS model. Section 3 presents the controllers for the two independent systems and then develops a coordination algorithm for the two inputs. Section 4 examines the performance of the integrated system and compares it with a vehicle using only ABS. The comparison will be done by means of a numerical simulation. Section 4 also determines constraints under which the systems must operate. These constraints include the maximum rate of increase/decrease for the brake torque as well as the maximum allowable normal force variation. A conclusion summarizes the main points of the paper.

2. System Models

Since the focus of this investigation is vehicle braking performance, the lateral dynamics of the vehicle

will be ignored. Consequently, only the longitudinal dynamics will be considered in the vehicle model. Therefore, an adequate model for this system is shown in Figure 2.1 below [17]:

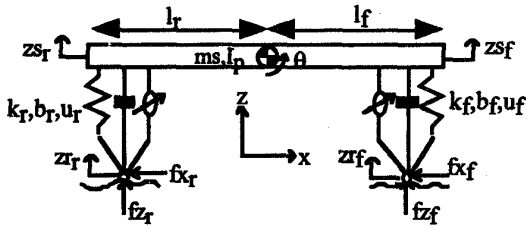


Figure 2.1
Half Car Model

Using the subscripts f & r to denote the front and rear, define:

- x : vehicle C.G. forward position
- z : vehicle C.G. vertical position
- I_p : vehicle pitch inertia about C.G.
- θ : vehicle pitch angle about C.G.
- h : height of C.G. from road
- z_r : road displacement
- z_s : sprung mass displ. from equilibrium
- k : suspension spring constant
- b : suspension damping constant
- u : active force element
- l_f : distance from C.G. to vehicle front wheel
- l_r : distance from C.G. to vehicle rear wheel

Using the above definitions, the dynamics of the Half Car Model can be represented by the following equations

$$\begin{aligned} m_s \ddot{x} &= -f_{x_f} - f_{x_r} \\ m_s \ddot{z} &= f_f + f_r \\ I_p \ddot{\theta} &= f_f l_f - f_r l_r - f_{x_f} (z_{s_f} - z_{r_f} + h) - f_{x_r} (z_{s_r} - z_{r_r} + h) \end{aligned} \quad (2.1)$$

where the suspension forces are defined as

$$\begin{aligned} f_f &= -k_{s_f} (z_{s_f} - z_{r_f}) - b_{s_f} (\dot{z}_{s_f} - \dot{z}_{r_f}) + u_f \\ f_r &= -k_{s_r} (z_{s_r} - z_{r_r}) - b_{s_r} (\dot{z}_{s_r} - \dot{z}_{r_r}) + u_r \end{aligned} \quad (2.2)$$

Assuming small angle deflections, the front and rear sprung mass positions can be approximated as

$$\begin{aligned} z_{s_f} &= z + l_f \theta \\ z_{s_r} &= z - l_r \theta \end{aligned} \quad (2.3)$$

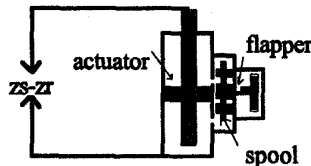


Figure 2.2
Electro-Hydraulic Suspension Actuator

The actuators that provide the suspension input forces, u , in Equation 2.2 are hydraulic pistons controlled by two-stage electro-hydraulic servovalves. A schematic

of such an actuator is shown in Figure 2.2. The actuators are controlled by a spool valve which is, in turn, controlled by the current input to a flapper valve with a force feedback spring. A detailed analysis of this type of device is given in Merritt [11]. The dynamics from input current to spool valve displacement are usually modeled as being third order. However, for the purpose of simplification, the two 'fast' poles of the flapper valve are ignored and only the dominant response pole of the spool is considered[5]. An analysis of this is given in [1]. Define:

x_v = spool valve displacement

τ = time constant

i = input current

P_L = actuator load pressure

P_s = supply pressure

A = actuator piston area

α, β, γ = hydraulic parameters

Using the above definitions the dynamics of the servovalve then become:

$$\dot{x}_v = \frac{1}{\tau} (-x_v + i) \quad (2.4)$$

and those of the actuator become

$$\dot{P}_L = -A\alpha(z_s - z_r) - \beta P_L + \gamma x_v \sqrt{P_s - \text{sign}(x_v) P_L} \quad (2.5)$$

The model of the ABS system can be developed by considering Figure 2.3.

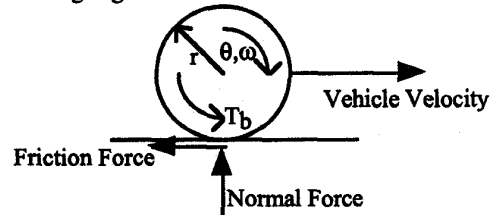


Figure 2.3
Wheel Coordinates and Forces

Define:

$v = \dot{x}$ = vehicle longitudinal velocity

ω = wheel angular velocity

T_b = brake torque from disks/drums

J = wheel inertia (including any drivetrain effects)

r = effective tire radius

N = normal force on the road

μ = coefficient of friction

λ = wheel slip

The equation of motion for the wheel is

$$\begin{aligned} J\dot{\omega} &= \text{Friction Force} \cdot r - T_b \\ &= \mu N r - T_b \end{aligned} \quad (2.6)$$

The coefficient of friction, μ , is a function of the wheel slip, λ , which is defined as

$$\lambda = \frac{v - \omega r}{v} \quad (2.7)$$

The relationship between μ and λ is given in a typical 'mu-slip' curve shown below.

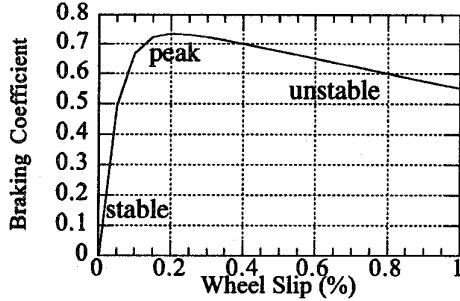


Figure 2.4
Friction Braking Coefficient vs. Wheel Slip
(Dry Asphalt)

The 'mu-slip' curve can be conveniently approximated by the function

$$\mu(\lambda) = a \cdot (1 - e^{-b\lambda}) - c\lambda \quad (2.8)$$

where

a = approximate peak friction value

b = approximate slope of curve's stable region

c = approximate slope of curve's unstable region

The reader is referred to [6] for additional analysis of 'mu-slip' curves and ABS systems. The objective of the ABS system is to keep the wheel slip close to the value which generates the peak friction coefficient.

3. Controllers

At each wheel, the objective for the ABS system modeled in Section 2 is to keep the wheel slip (λ) close to the peak value (λ_{peak}) on the 'mu-slip' curve. One control approach to meet this objective is a variable-structure controller presented in Tan[16]. The dynamics of the brake actuator can be modeled as a first order system shown below:

$$\dot{T}_b = \begin{cases} C_{\text{fill}}(-T_b + K_b u_b) & \text{fill stage} \\ C_{\text{dump}}(-T_b + K_b u_b) & \text{dump stage} \end{cases} \quad (3.1)$$

where C_{fill} and C_{dump} represent the time constants of the brake cylinder's fill and dump phases. This model does not include the hold phase of the brake cylinder. u_b is a constant supply pressure that is regulated by an on-off solenoid valve. The brake gain K_b is a function of brake radius, brake pad friction coefficient, brake temperature, and number of pads. K_b converts the brake pressure to brake torque. The control strategy for the ABS system is a simple variable structure controller operating within a boundary layer about the peak wheel slip value.

$$K_b u_b(t) = \begin{cases} M & \forall \lambda < \lambda_{\text{peak}} - \frac{\epsilon}{2} \\ 0 & \forall \lambda > \lambda_{\text{peak}} + \frac{\epsilon}{2} \\ K_b u_b(t - \Delta t) & \forall |\lambda - \lambda_{\text{peak}}| < \frac{\epsilon}{2} \end{cases} \quad (3.2)$$

The boundary layer with magnitude ϵ is introduced to avoid control chattering about λ_{peak} and Δt is the controller sampling time.

The force tracking control for the electro-hydraulic active suspension has been detailed in Alleyne & Hedrick [1] for the quarter car model. If the desired force profile (F_{desired}) is specified, the desired actuator load pressure ($P_{L\text{desired}}$) is simply F_{desired}/A . Given the model of the actuator in Equations (2.4) and (2.5) a two stage feedback linearization controller can be developed using the method of synthetic inputs [2,7].

$$x_{\text{vdesired}} = \frac{A\alpha(\dot{z}_s - \dot{z}_r) + \beta P_L + \dot{P}_{L\text{desired}} - k_1(P_L - P_{L\text{desired}})}{\gamma\sqrt{P_s} - \text{sign}(x_v)P_L} \quad (3.3)$$

$$\dot{i} = x_v + \tau(\dot{x}_{\text{vdesired}} - k_2(x_v - x_{\text{vdesired}}))$$

A desired value of spool displacement is determined and the actual current input is used to achieve this.

The coordination of the two inputs, described by Equations (3.2) and (3.3), will be developed and implemented separately at each wheel. Therefore, there will be no coordination between the front and rear wheels. The normal force at each wheel is the sum of the suspension forces and the dynamic weight of the vehicle. The goal of the subsystem integration is to have the normal force on the tire change in phase with the brake torque being applied. When the brake torque is high, the normal force would be high and vice versa. The net effect is a perceived increase in normal tire force with no increase in vehicle inertia. The integration algorithm is represented by

$$F_{\text{desired}} = A \cdot \text{sign}(T_b - \bar{T}_b) \quad (3.5)$$

with \bar{T}_b denoting the mean brake torque on the wheel during braking and A denoting the amplitude of the force desired from the active suspension actuator. The amplitude of the force cannot be made arbitrarily large since it affects the acceleration of the vehicle's sprung mass. A tradeoff must be made between allowable sprung mass acceleration and normal force variation. This will be done in Section 4.

Simulation Results

The values used in the simulations are given below [1,16,17].

$$\begin{aligned} m_s &= 730.0 \text{ kg} & I_p &= 1230.0 \text{ kg-m}^2 \\ r &= 0.3 \text{ m} & J_f &= 1.4 \text{ kg-m}^2 \end{aligned}$$

$J_r = 1.0 \text{ kg-m}^2$ $ks_f = 19960.0 \text{ N/m}$
 $ks_r = 17500.0 \text{ N/m}$ $bs_f = 1050.0 \text{ N-s/m}$
 $bs_r = 900.0 \text{ N-s/m}$ $l_f = 1.011 \text{ m}$
 $l_r = 1.803 \text{ m}$ $h = 0.508 \text{ m}$
 $\alpha = 4.515e13 \text{ N/m}^5$ $\beta = 1.0$
 $\gamma = 1.54e9 \text{ N/m}^{5/2} \text{ kg}^{1/2}$ $\tau = 0.003$
 $P_s = 10342500.0 \text{ Pa}$ $A = 3.35e-4 \text{ m}^2$
 $M = 2000 \text{ N-m}$ $C_{fill} = 15.0$
 $C_{dump} = 15.0$ $a = 0.5$
 $b = 20.0 \text{ 1/s}$ $c = 0.2$

The road surface corresponds wet asphalt. The magnitude of the maximum allowable sprung mass acceleration is limited to be $\pm 0.3 \text{ g's}$. As a result, the maximum amplitude of force from the active suspension actuator is determined to be 1000.0 N . The initial velocity of the vehicle is 16 m/s or approximately 35 mph . Figure 4.1 shows the position vs. time of a vehicle using just ABS.

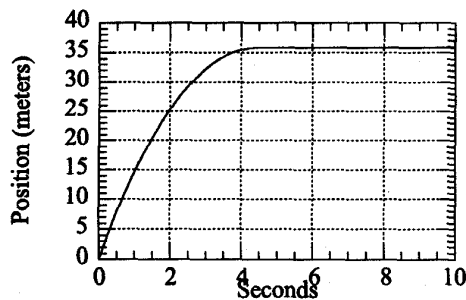


Figure 4.1
(ABS) Vehicle Position

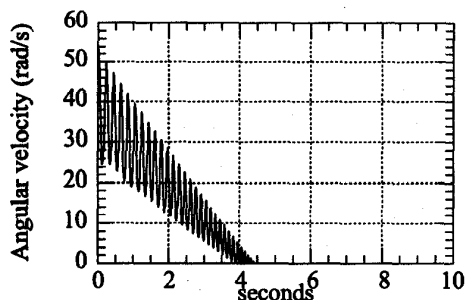


Figure 4.2
(ABS) Front Wheel Speed

Figure 4.2 shows the wheel speed of the vehicle for the front wheel only. The data for the rear wheel is similar and is not shown here. This figure clearly shows the regions of increasing and decreasing wheel slip which correspond to the filling and dumping of the brakes. Figure 4.3 shows the brake torque being applied to the front wheel. As in Figure 4.2, the data for the rear wheel is similar and is not shown here.

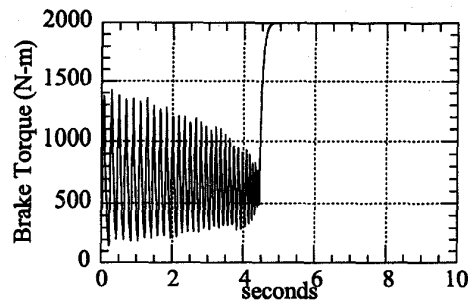


Figure 4.3
(ABS) Front Brake Torque

Since there is no active suspension force in this case, the variation in normal force on the road is purely a function of the dynamic weight transfer. The front tire normal force is shown in Figure 4.4.

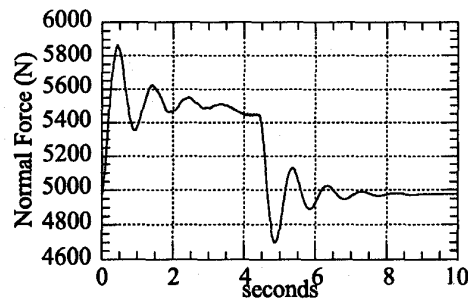


Figure 4.4
Front Tire Normal Force

The dynamic weight transfer is from front to rear so the rear tire normal force would be the reflection of Figure 4.4 about the equilibrium force ($\sim 5000 \text{ N}$) shown at $t = 10$ seconds. The rear tire normal force is not shown here.

Figure 4.5 shows the longitudinal vehicle position with the integrated (ABS & Active Suspension) control approach.

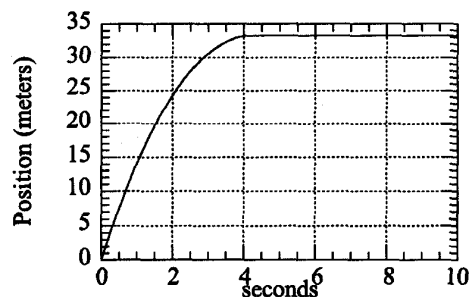


Figure 4.5
(Integrated) Vehicle Position

Using the integrated approach, the braking distance is reduced by $\sim 7\text{-}8\%$ over just ABS. The wheel speeds are quite similar to Figure 4.2 and are not shown. Figure

4.6 shows the front wheel brake torque and normal force on the same graph. As is seen in the figure, the brake torque and the normal force variation are in phase which leads to the reduction in stopping distance shown in Figure 4.5.

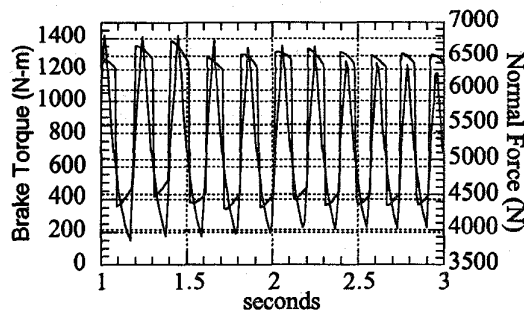


Figure 4.6
(Integrated)
Brake Torque and Normal Force

Conclusion

This paper has developed an algorithm for integrating two components of the vehicle's chassis that would otherwise operate independently. A Half Car model of a vehicle was introduced along with model of an ABS system and an Active Suspension System. Two separate controllers were developed for the ABS and the Active Suspension. The controllers were then coordinated by having the desired force profile of the suspension actuator be a function of the brake actuator's performance. The integrated approach was simulated along with an ABS approach. For the allowable sprung mass acceleration, the integrated control provided an 8 percent decrease in stopping distance on a given surface. Additionally, the frequency of the suspension actuator force is well above the natural frequency of the sprung mass. Therefore, although the sprung mass acceleration is affected, the other suspension states are not greatly affected.

References

- [1] Alleyne, A., and Hedrick, J.K., "Nonlinear Adaptive Control of Active Suspensions," *IEEE Transactions on Control Systems Technology*, Vol. 3, No.1, March 1995.
- [2] Alleyne, A., and Hedrick, J.K., "Application of Nonlinear Control Theory to Electronically Controlled Suspensions," *Vehicle System Dynamics*, Vol. 22, 1993, pp. 309-320.
- [3] Buschmann, G., Ebner, H.T., and Kuhn, W., "Electronic Brake Force Distribution Control - A Sophisticated Addition to ABS," SAE Paper 920646, *ABS/Traction Control and Advanced Brake Systems*, SP-914, pp. 93-100, February, 1992.
- [4] Dreyer, A., Graber, J., Hoffman, M., Rieth, P., Schmitt, S., "Structure and Function of the Brake and Suspension Control System, BSCS," *IMEchE No. C389/306 or FISITA No. 925078, Proc. of the XXIV FISITA Congress*, London, pp. 7-18, June 1992.
- [5] Engleman G.H., and Rizzoni, G., "Including the Force Generation Process in Active Suspension Control Formulation," *Proc. of the 1993 ACC*, San Francisco CA, June 1993, pp. 701-705.
- [6] Gillespie, T.D., *Fundamentals of Vehicle Dynamics*, SAE Press, 1992.
- [7] Green, J. and Hedrick, J.K., "Nonlinear Speed Control for Automotive Engines," *Proc. of the 1990 ACC*, San Diego CA, June 1990, pp. 2891-2897.
- [8] Kimbrough, S. and VanMoorhem, W., "A Control Strategy for Stabilizing Trailers via Selective Actuation of Brakes," DSC-Vol 44, Transportation Systems, *Proceedings of the 1992 ASME Winter Annual Meeting (WAM)*, Anaheim, CA, November 1992, pp. 413-428.
- [9] Matsumoto, S., Yamaguchi, H., Inoue, H., and Yasuno, Y., "Improvement of Vehicle Dynamics Through Braking Force Distribution Control," SAE Paper 920645, *ABS/Traction Control and Advanced Brake Systems*, pp. 83-92, *Proc. of the 1992 SAE International Congress and Exposition*, SP-914, Detroit, MI, February, 1992.
- [10] Matsumoto, N., and Tomizuka, M., "Vehicle Lateral Velocity and Yaw Rate Control with Two Independent Control Inputs," *ASME Journal of Dynamic Systems, Measurement and Control*, Vol. 114, pp. 606-613, December 1992.
- [11] Merritt, H.E., *Hydraulic Control Systems*, John Wiley & Sons, 1967.
- [12] Miyasaki, N., Fukumoto, M., Sogo, Y., Tsukinoki, H., "Antilock Brake System (M-ABS) Based on the Friction Coefficient Between the Wheel and the Road Surface," SAE Paper 900207, *ABS Traction Control and Brake Components*, pp. 101-110, *Proc. of the 1990 SAE International Congress and Exposition*, Detroit, MI, February 1990.
- [13] Motoyama, S., Uki, H., Isoda, K., Yuasa, H., "Effect of Traction Force Distribution Control on Vehicle Dynamics," *Vehicle System Dynamics*, Vol. 22, pp. 455-464, 1993.
- [14] Nadol, M., "Computer Simulation of an Anti-Lock Brake System with Emphasis on the Effects of Drivetrain Configurations on System Operation," M.S. Thesis, Department of Mechanical and Industrial Engineering, University of Illinois at Urbana-Champaign, June 1989.
- [15] Roppenecker, G., and Wallentowitz, H., "Integration of Chassis and Traction Control Systems: What is Possible - What Makes Sense - What is Under Development," *Vehicle System Dynamics*, Vol. 22, pp. 283-298, 1993.
- [16] Tan, H.S., "Adaptive and Robust Controls with Application to Vehicle Traction Control," Ph.D. Dissertation, Department of Mechanical Engineering, University of California at Berkeley, August 1988.
- [17] Tseng, H.E., "A Methodology for Optimizing Semi-Active Suspensions for Automotive Applications," Ph.D. Dissertation, Department of Mechanical Engineering, University of California at Berkeley, February 1994.
- [18] Xia, X., and Law, E.H., "Response of Four-Wheel-Steering Vehicles to Combined Steering and Braking Inputs," DSC-Vol 13, *Advanced Automotive Technologies, Proceedings of the 1992 ASME WAM*, San Francisco, CA, December 1989, pp. 107-128.